# New Test Method for Determining Energy Absorption Mechanisms in Polymer Composite Plates

GEORGE C. JACOB*

*Materials Science and Engineering Department*
*University of Tennessee, Knoxville*
*434 Dougherty Engineering*
*Knoxville, TN 37996*

J. MICHAEL STARBUCK

*Polymer Matrix Composites Group*
*Metals and Ceramics Division*
*Oak Ridge National Laboratory*
*Post Office Box 2009*
*Oak Ridge, TN 37831-8048*

SRDAN SIMUNOVIC

*Computational Material Science*
*Computer Science and Mathematics Division*
*Oak Ridge National Laboratory*
*Post Office Box 2008, Bldg. 6025, MS-6359*
*Oak Ridge, TN 37831-6359*

JOHN F. FELLERS

*Materials Science and Engineering Department*
*University of Tennessee, Knoxville*
*608 Dougherty Engineering*
*Knoxville, TN 37996*

In passenger vehicles the ability to absorb energy due to impact and be survivable to the occupant is called the "crashworthiness" of the structure. To identify and quantify the energy absorbing mechanisms in candidate automotive composite materials, test methodologies were developed for conducting progressive crush tests on composite plate specimens. The test method development and experimental setup focused on isolating the damage modes associated with frond formation that occurs in dynamic testing of composite tubes. A new test fixture was designed to progressively crush composite plate specimens under quasi-static test conditions. Features incorporated into the design include an observable crush zone, long crush length, interchangeable contact profile, frictionless roller for contact constraint, and out of plane roller supports to prevent buckling. Preliminary results are presented under a sufficient set of test conditions to validate the operations of the test fixture. The activation of different damage mechanisms was demonstrated by the validation tests on the representative composite material systems. The experimental data, in conjunction with test observations will be used in future work to identify the characteristic damage and failure modes, and determine the energy absorption capability of candidate automotive composite material systems.

*To whom correspondence should be addressed. E-mail: gjacob@utk.edu

## INTRODUCTION

In passenger vehicles the ability to absorb impact energy and be survivable for the occupant is called the "crashworthiness" of the structure. There is an important difference between crashworthiness and penetration resistance. Crashworthiness is concerned with the absorption of energy through controlled failure mechanisms and modes that enable the maintenance of a gradual decay in the load profile during absorption. Penetration resistance is associated with the total absorption without allowing projectile or fragment penetration. The crashworthiness of a material is expressed in terms of its specific energy absorption, SEA, which is characteristic of that particular material. Specific energy absorption is defined as the energy absorbed per unit mass of material. Mathematically SEA = $\sigma/\rho$, where $\rho$ is the density of the composite material and $\sigma$ is the mean crush stress.

Current legislation for automobiles requires that vehicles be designed such that, in the event of an impact at speeds up to 15.5 m/sec (35 mph) with a solid, immovable object, the occupants of the passenger compartment should not experience a resulting force that produces a net deceleration greater than 20 g (1). Crashworthy structures should be designed to absorb impact energy in a controlled manner, thereby bringing the passenger compartment to rest without the occupant being subjected to high decelerations, which can cause serious internal injury, particularly brain damage.

Vehicle size and mass provide a certain degree of protection but can have negative inertial effects. Driven by the need to overcome these negative effects of both size and mass coupled with mandates for increased fuel efficiency, an attempt is being made to use composites in the development of energy dissipating devices. The ability to tailor composites, in addition to their attributes of high stiffness-to-weight and strength-to-weight ratios, fatigue resistance and corrosion resistance, makes them very attractive in crashworthiness. The challenge is the use of specific features of geometry and materials in enabling greater safety while simultaneously decreasing the weight, without negatively affecting the overall economics of fabrication and production.

To reduce the overall weight and improve the fuel economy of vehicles, more and more metal parts are being replaced by polymer composite materials. Contrary to metals, especially in compression, most composites are generally characterized by a brittle rather than ductile response to load. While metal structures collapse under crush or impact by buckling and/or folding in accordion (concertina) type fashion involving extensive plastic deformation, composites fail through a sequence of fracture mechanisms involving fiber fracture, matrix crazing and cracking, fiber-matrix debonding, de-lamination and inter-ply separation. The actual mechanisms and sequence of damage are highly dependent on the geometry of the structure, lamina orientation, type of trigger and crush speed, all of which can be suitably designed to develop high energy absorbing mechanisms. Much of the experimental work to study the effects of fiber type, matrix type, fiber architecture, specimen geometry, processing conditions, fiber volume fraction and testing speed on the energy absorption of composite materials has been carried out on axisymmetric tubes (2–45). Tube structures are relatively easy to fabricate and close to the geometry of the actual crashworthy structures.

In the progressive crushing of composite tubes there are many different failure mechanisms that contribute to the overall energy absorption of the structure. To isolate the damage mechanisms and quantify the energy absorption contributed by the splaying mode, a unique test fixture was designed and used for testing composite plate specimens. Practical considerations related to the cost of production of the test specimens were of paramount importance in developing the test methodology. Composite plate specimens are very cheap to fabricate and it has been observed that plate specimens progressively crush in modes very similar to the damage modes that occur during progressive crushing of composite tubes. Also plates can be easily produced with consistently high quality.

## TEST FIXTURE DESIGN

A new test fixture design was developed for determining the deformation behavior and damage mechanisms that occur during progressive crushing of composite materials. The fixture was designed to isolate the damage modes associated with the frond formation (splaying mode) in composite tubes by testing plate geometries. The fixture can be used in conventional screw driven or hydraulically actuated load frames and is intended for quasi-static loading but may be adaptable to conducting dynamic tests with minor modifications. The design of the test fixture can accommodate different plate widths (up to 50 mm), plate thicknesses (nominally 3 mm ± 1.55 mm), contact profile shapes, and contact profile constraints.

The design is a modified version of an existing test fixture used for crush testing of composite plates (46). Features incorporated into the design include an observable crush zone, long crush length, interchangeable contact profile, frictionless roller for contact constraint, and out of plane roller supports to prevent buckling. A schematic of the test fixture is shown in *Fig. 1* and photos are shown in *Fig. 2* and *Fig. 3*. Below is a list of the primary components of the fixture (see *Fig. 1*).

1. Top plate
2. Base plate
3. Profile block
4. Roller plate
5. Grip plate and insert
6. Linear shaft and bearing
7. Load cell
8. Roller way

The composite plate specimen is clamped in the top plate by the grip inserts. The specimen is then loaded in compression and crushed through the contact profile as defined by the profile block via the top plate that is connected to the load train using a shaft coupler.

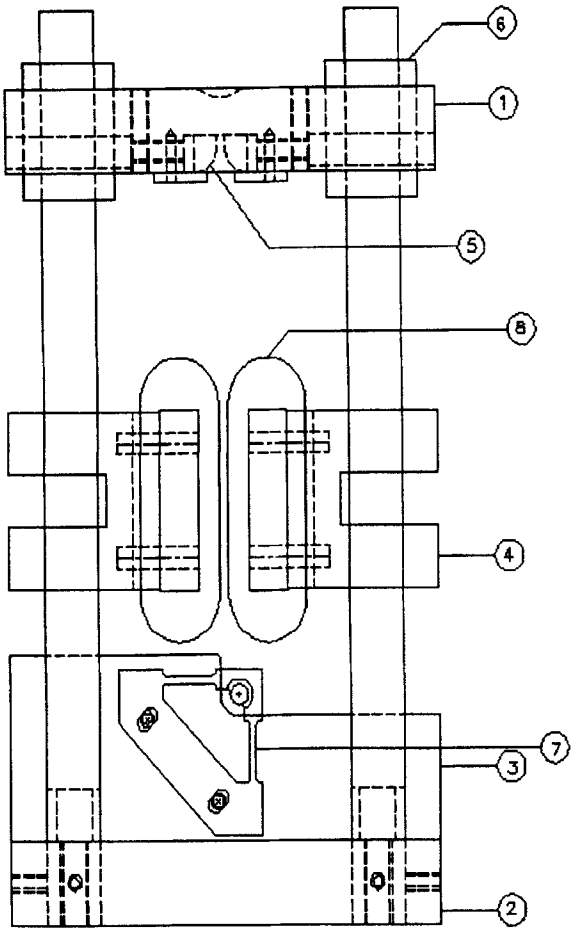


Fig. 1. Schematic of test fixture design.

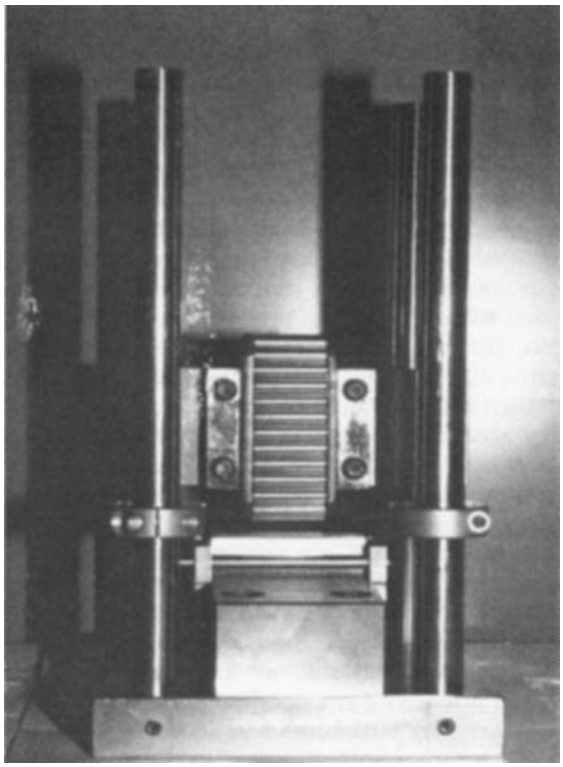

Fig. 2. Roller ways and contact profile constraint—1.

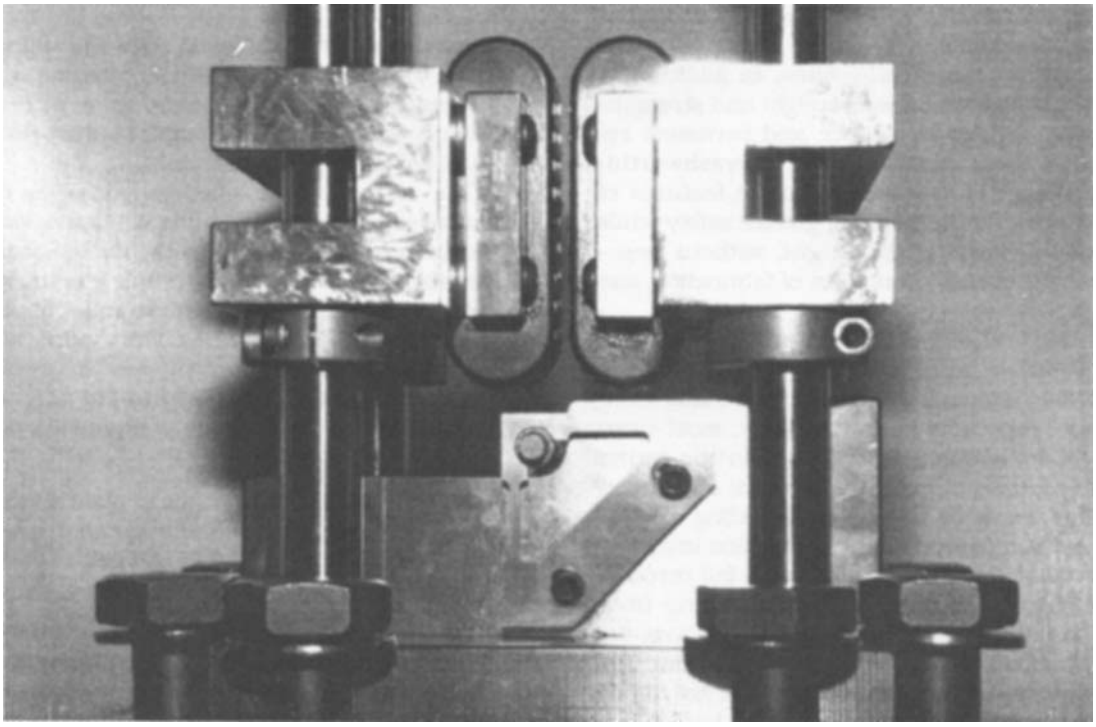

Fig. 3. Roller ways and contact profile constraint—2.

The top plate is displaced downward, relative to the base plate and profile block. Alignment is maintained by using four linear shafts and linear bearings. Attached to the roller plates that are positioned on the linear shafts by shaft collars are the roller ways. The roller ways are used to reduce the unsupported length of the specimen thereby preventing the specimen from buckling. The brackets on either side of the profile plate were designed to serve two functions. The first function is to provide a method of constraining the specimen to deform along the path of the contact profile. Using oil-impregnated bronze sleeve bearings in each bracket and installing a precision ground shaft that acts as a roller accomplish this. The second function is a development effort to measure the vertical and horizontal reaction forces experienced by the specimen during the deformation process. The severity of the contact profile constraint is determined by the position of the load cell brackets and is adjustable using slotted positioning holes. See *Fig. 4*. Slotted holes are used throughout the test fixture design to accommodate different plate thicknesses and maintain alignment with the centerline of the load train.

## VARIABLE EFFECTS INVESTIGATING CAPABILITY

The fixture was designed to study the effects plate width, loading rate, profile constraint and profile shape have on the energy absorbing characteristics of composite plates. Furthermore, the objective of the profile constraint was to determine if different damage mechanisms could be activated depending on the position of the roller. Below is a summary of the various variables whose effects the fixture is capable of investigating.

- Profile Radius: 6.4 mm (0.25 inch) and 13 mm (0.5 inch)
- Loading Rate: 5 mm/min (0.2 inches/min) and 50 mm/min (2 inches/min)
- Constraint: None, Loose, Tight
- Plate Width: 13 mm (0.5 inch), 25.4 mm (1 inch), 50 mm (2 inches)

## FIXTURE VALIDATION

The material systems that were tested for validating the test fixture included a graphite/epoxy cross-ply laminate and a graphite epoxy braided material. The cross-ply laminate was fabricated using the hand lay-up process and Akzo Fortafil Prepreg #602. There were two plates fabricated, designated as CP#1 and CP#2, where the CP#2 plate was not adequately consolidated because of loosing vacuum pressure partially through the cure cycle. The graphite/epoxy braided specimens were fabricated using Akzo #556 carbon fiber with Ashland Hetron 922 epoxy vinyl ester. The lay-up was a triaxial braid with $0/+30°/-30°$ fiber orientations and the panel designation was 'O'.

All the specimens had a nominal length of 178 mm. The cross-ply laminates (CP#1 and CP#2) and the triaxial braided specimens had a width of 50 mm and 38 mm respectively and a 45° chamfer was used as the crush initiator. A diamond cutoff wheel was used to the cut the specimens off the composite panel. No coolant was used during cutting to prevent contamination of the test specimens. A loading rate of 5.0 mm/min and a profile block of radius equal to 6.4 mm was used through out the entire testing.

The MTS machine (Model 810, axial/torsional mode) used for testing had a load capacity of 50,000 lbs. The load-deflection response was recorded using a computerized data acquisition system. A 16 bit, 100 kHz National Instrument data acquisition card numbered pci6031E was used. The area under the load deflection curve was the total energy absorbed and the initial peak load and sustained crush load were identified.

The specific energy absorption, SEA, of a composite material defined as the energy absorbed per unit mass of the material is equal to W/m where 'W' is the total energy absorbed in crushing of the composite plate specimen which is the area under the load-displacement curve and 'm' is the mass of the specimen. From SEA = W/m, one can write SEA = W/Vρ, where 'V' is the volume of the crushed portion of the composite plate specimen and 'ρ' is the density of the composite material. One can also write SEA = W/(ALρ), where 'A' and 'L' are the cross-sectional area and length of the

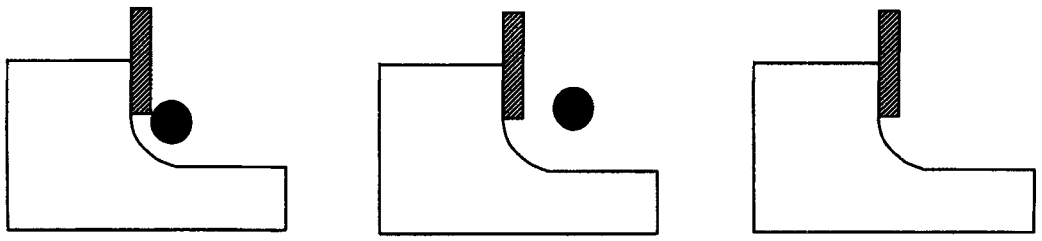


*Fig. 4. Constraint conditions.*

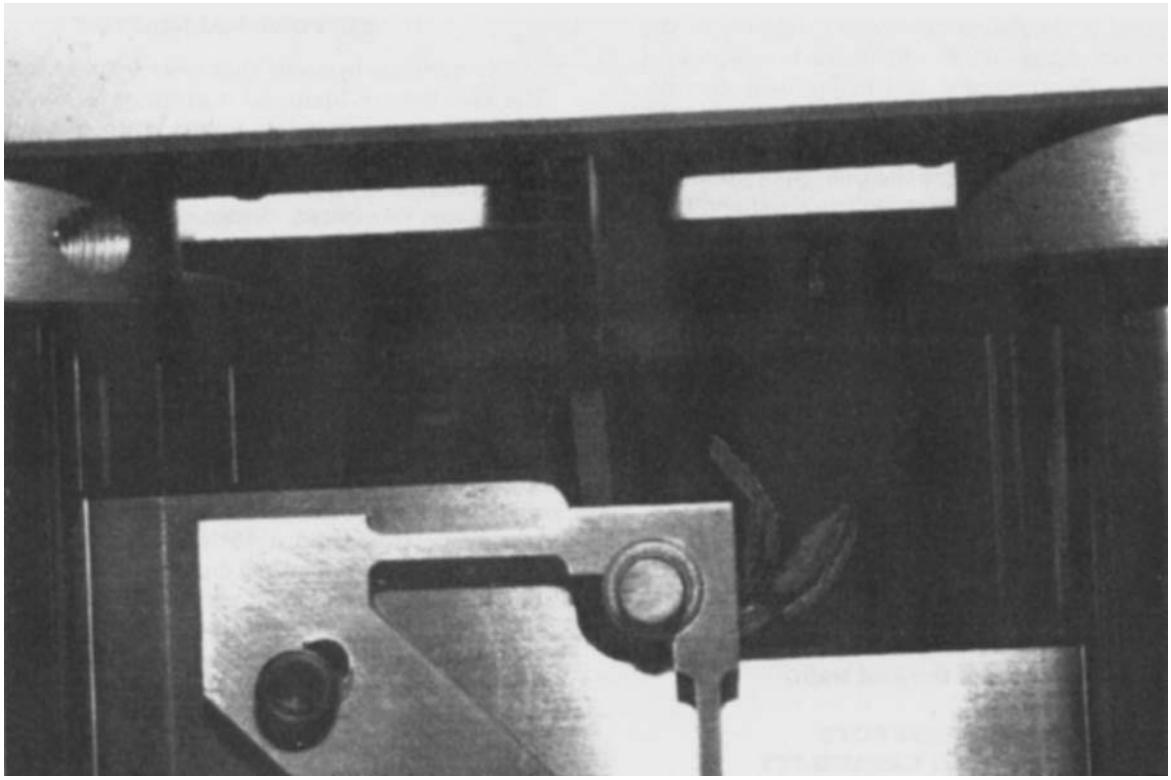

*Fig. 5. Crushing of a CP#1 specimen.*

crushed portion of the composite plate specimen respectively. SEA = W/(ALρ) was used to calculate the specific energy absorption of all the composite plate specimens tested. *Figure 5* shows the crushing of a CP#1 specimen plate when loaded in compression.

### Graphite/Epoxy Cross Ply Laminate: CP#1

The experimental data from the measured load-deflection responses are summarized in *Table 1*.

For the CP#1 cross-ply panels the no constraint condition resulted in the highest initial peak load and the highest maximum peak load relative to the other constraint conditions. See *Table 1*. For a comparison of the load displacement traces recorded for a test conducted on a specimen in the no constraint, the loose constraint, and the tight constraint condition, respectively, see *Fig. 6*.

The predominant damage mechanism for the cross-ply plate was delamination. See *Fig. 7* and *Fig. 8*. The

**Table 1. Experimental Data for CP#1.**

| Specimen Number | Specimen Width (cm) | Profile Radius (cm) | Constraint | Initial Peak Load (N) | Max. Peak Load (N) | Sustained Crush Load (N) | SEA (J/g) | Avg. SEA (J/g) |
|---|---|---|---|---|---|---|---|---|
| CP1-1 | 5.072 | 0.635 | None | 5491.1 | 7982.2 | 5280.7 | 11.12 | |
| CP1-2 | 5.075 | 0.635 | None | 7561.4 | 7806.0 | 4372.8 | 13.65 | |
| CP1-3 | 5.073 | 0.635 | None | 7501.5 | 7814.2 | 5102.3 | 12.73 | 12.38 |
| CP1-4 | 5.073 | 0.635 | None | 7545.6 | 7825.7 | 5110.3 | 12.83 | |
| CP1-5 | 5.070 | 0.635 | None | 6555.5 | 7880.6 | 5274.3 | 11.57 | |
| CP1-6 | 5.070 | 0.635 | Loose | 4534.2 | 4975.5 | 3580.5 | 19.81 | |
| CP1-7 | 5.072 | 0.635 | Loose | 4615.4 | 7758.4 | 4194.8 | 21.58 | |
| CP1-8 | 5.075 | 0.635 | Loose | 3807.8 | 5688.2 | 3505.8 | 13.65 | 18.36 |
| CP1-9 | 5.075 | 0.635 | Loose | 4580.3 | 5588.7 | 3977.7 | 18.69 | |
| CP1-10 | 5.070 | 0.635 | Loose | 4576.3 | 5576.8 | 3856.6 | 18.07 | |
| CP1-11 | 5.065 | 0.635 | Tight | 4422.2 | 6238.4 | 5038.7 | 25.58 | |
| CP1-12 | 5.070 | 0.635 | Tight | 4400.5 | 6236.7 | 5009.3 | 25.00 | |
| CP1-13 | 5.073 | 0.635 | Tight | 4435.6 | 6300.6 | 5040.7 | 25.79 | 25.56 |
| CP1-14 | 5.069 | 0.635 | Tight | 4418.5 | 6199.3 | 5028.3 | 25.51 | |
| CP1-15 | 5.070 | 0.635 | Tight | 4446.3 | 6246.6 | 5045.2 | 25.91 | |

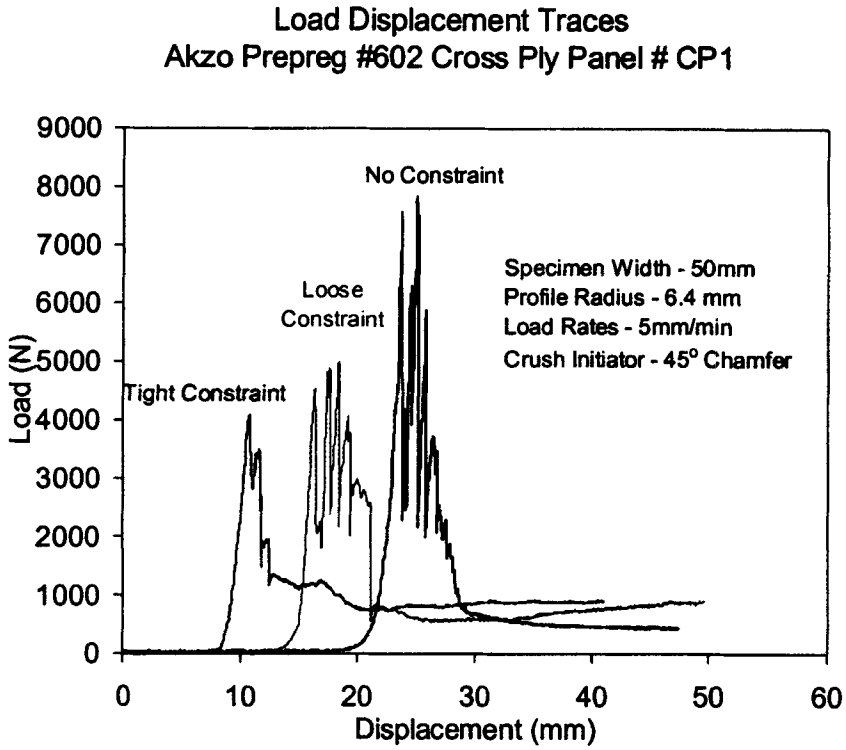


*Fig. 6. Load displacement traces for CP#1.*

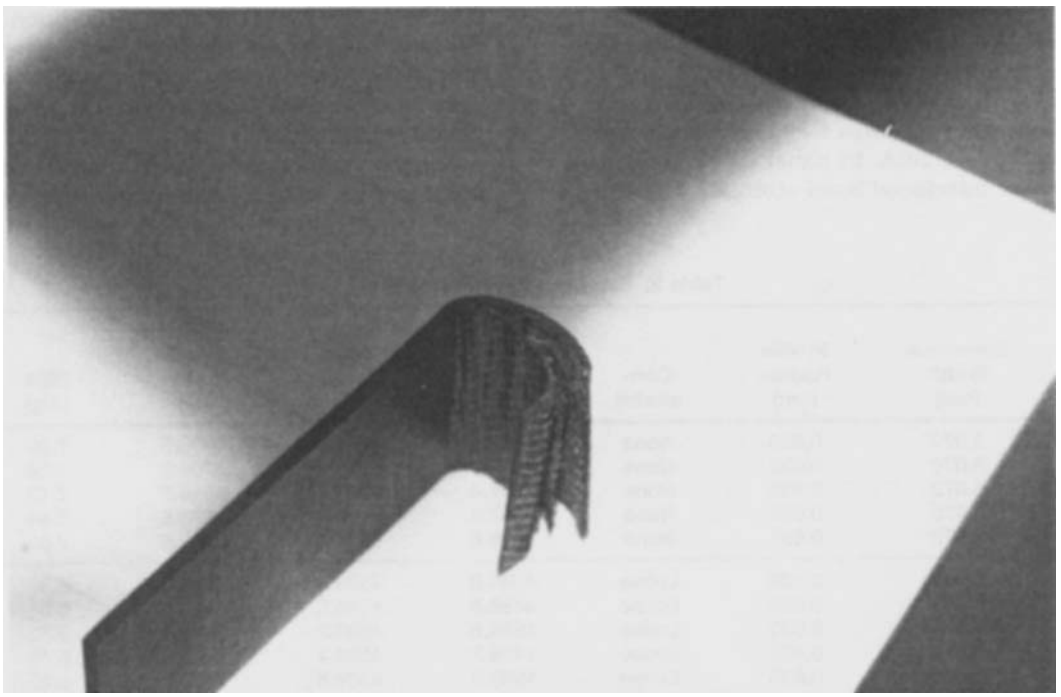

*Fig. 7. Crushed CP#1 specimen—1.*

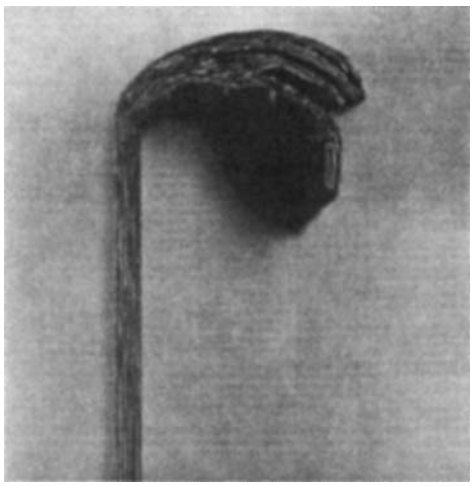

*Fig. 8. Crushed CP#1 specimen—2.*

constraint condition influenced the damage mechanisms. Tight constraint to loose constraint to the no constraint condition resulted in larger delamination growths, larger number of delaminations, and greater permanent deformations. The plateau in the load deflection responses (see *Fig. 6*) corresponded to complete delamination between all the layers.

The specific energy absorption, SEA, was highest in the tight constraint condition. No constraint to loose constraint to tight constraint resulted in larger specific energy absorption, SEA (see *Table 1*).

### Graphite/Epoxy Cross-Ply Laminate: CP#2

The experimental data from the measured load-deflection responses are summarized in *Table 2*.

The panel CP#2 had significantly lower SEA's than panel CP#1. Compared to panel CP#1, the lower specific energy absorption, SEA, in panel CP#2 is attributed to the weaker interfacial bond strength, resulting from poor consolidation, requiring less energy to delaminate.

For the CP#2 cross-ply panels the no constraint condition resulted in the highest initial peak load and the highest maximum peak load relative to the other constraint conditions. See *Table 2*. For a comparison of the load displacement traces recorded for a test conducted on a specimen in the no constraint, the loose constraint, and the tight constraint condition, respectively, see *Fig. 9*.

The predominant damage mechanism for the cross-ply plate was delamination. See *Fig. 10* and *Fig. 11*. The constraint condition influenced the damage mechanisms. Tight constraint to loose constraint to the no constraint condition resulted in larger delamination growths, larger number of delaminations, and greater permanent deformations. The plateau in the load deflection responses (see *Fig. 9*) corresponded to complete delamination between all the layers.

For the panel CP#2, the specific energy absorption, SEA, was significantly higher for the tight constraint condition (see *Table 2*).

### Graphite/Epoxy Triaxial Braid with 0/+30°/−30° Fiber Orientations: O

The experimental data from the measured load-deflection responses are summarized in *Table 3*.

For the braided material the no constraint condition resulted in a higher initial peak load relative to the loose constraint condition. The no constraint condition however resulted in a lower sustained crush load relative to the loose constraint condition. See *Table 3*. For a comparison of the load displacement traces recorded for a test conducted on a specimen in the no constraint and the loose constraint condition, respectively, see *Fig. 12*.

For the braided material, the active damage mechanisms were localized crushing, fiber fracture on the

**Table 2. Experimental Data for CP#2.**

| Specimen Number | Specimen Width (cm) | Profile Radius (cm) | Constraint | Initial Peak Load (N) | Max. Peak Load (N) | Sustained Crush Load (N) | SEA (J/g) | Avg. SEA (J/g) |
|---|---|---|---|---|---|---|---|---|
| CP2-1 | 5.072 | 0.635 | None | 5962.1 | 6103.8 | 3970.5 | 7.89 | |
| CP2-2 | 5.070 | 0.635 | None | 4309.9 | 6721.9 | 3259.2 | 7.08 | |
| CP2-3 | 5.072 | 0.635 | None | 5091.4 | 6532.2 | 3546.7 | 7.13 | 7.47 |
| CP2-4 | 5.075 | 0.635 | None | 4967.2 | 6109.4 | 3876.5 | 7.44 | |
| CP2-5 | 5.072 | 0.635 | None | 5876.6 | 6675.4 | 3969.6 | 7.81 | |
| CP2-6 | 5.080 | 0.635 | Loose | 4594.8 | 4594.8 | 2175.5 | 6.33 | |
| CP2-7 | 5.055 | 0.635 | Loose | 4436.8 | 4436.8 | 1463.1 | 6.86 | |
| CP2-8 | 5.076 | 0.635 | Loose | 4595.8 | 4590.2 | 1890.4 | 6.73 | 6.65 |
| CP2-9 | 5.075 | 0.635 | Loose | 4496.7 | 4593.4 | 2172.3 | 6.48 | |
| CP2-10 | 5.060 | 0.635 | Loose | 4509.8 | 4509.8 | 1987.2 | 6.85 | |
| CP2-11 | 5.075 | 0.635 | Tight | 4670.1 | 6000.2 | 4618.5 | 20.10 | |
| CP2-12 | 5.075 | 0.635 | Tight | 4582.6 | 4582.6 | 3020.1 | 15.13 | |
| CP2-13 | 5.074 | 0.635 | Tight | 4600.8 | 4600.8 | 3600.9 | 16.13 | 17.60 |
| CP2-14 | 5.075 | 0.635 | Tight | 4656.6 | 5890.7 | 4456.7 | 19.12 | |
| CP2-15 | 5.075 | 0.635 | Tight | 4592.3 | 5803.4 | 4278.5 | 17.52 | |

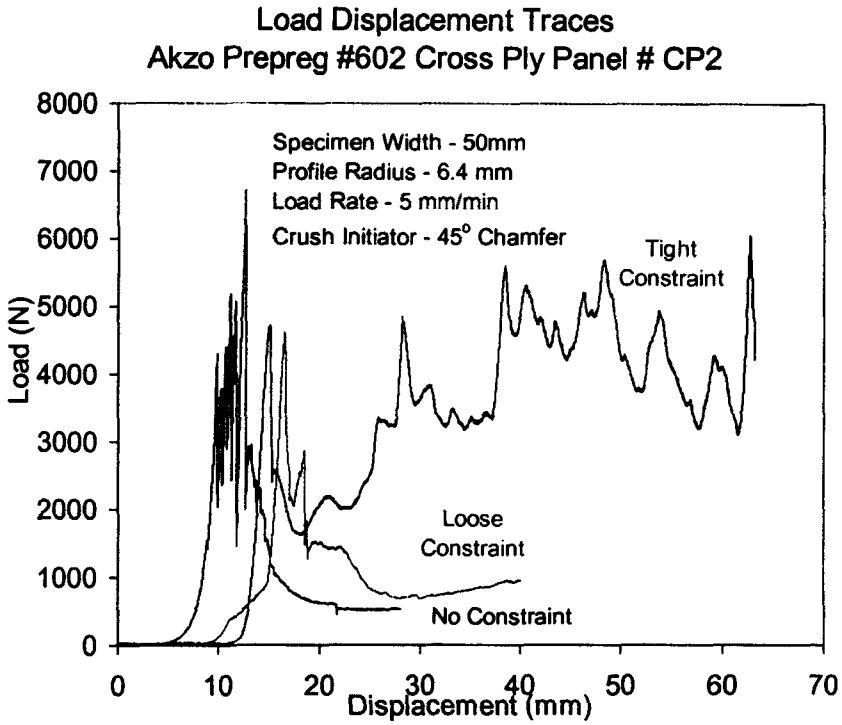


*Fig. 9. Load displacement traces for CP# 2.*

tensile side of the specimen, and fiber buckling of the off-axis tows on the compressive side of the specimen. The fiber buckling was more extensive when the no constraint condition was used, where as the fiber fracture was more predominant in the loose constraint tests.

The results of the braided material show higher specific energy absorption, SEA, when the loose condition was used compared to no constraint (see *Table 3*). The loose constraint condition produced a nearly ideal response for progressive crushing, as can be seen in *Fig. 12*.

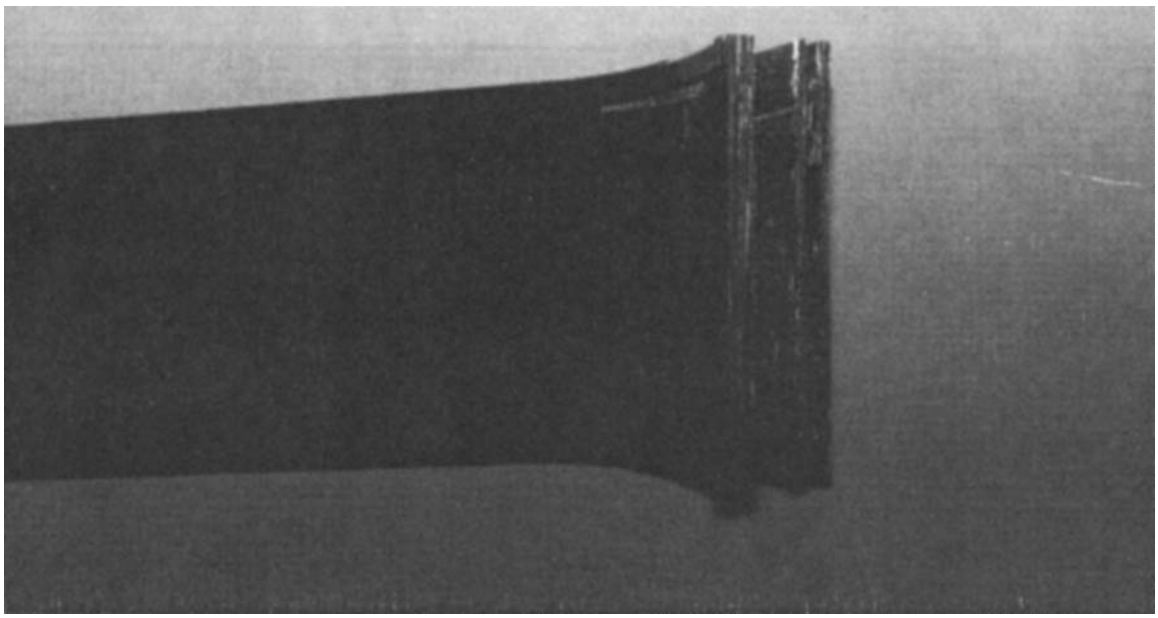

*Fig. 10. Crushed CP# 2 specimen—1.*

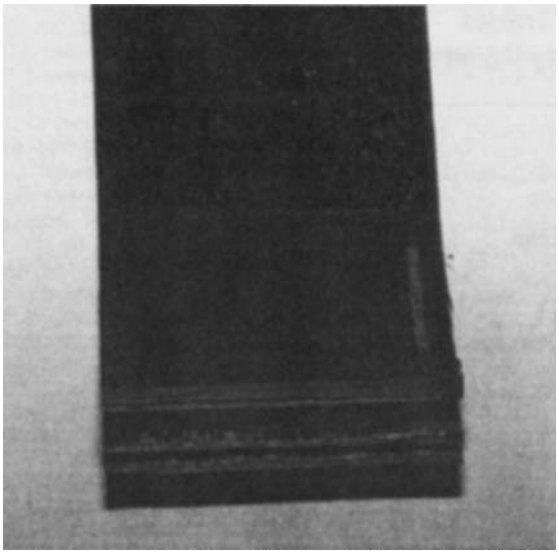

*Fig. 11. Crushed CP# 2 specimen—2.*

## CONCLUSION

A unique test fixture was developed for determining the energy absorbing mechanisms in automotive composite material systems. The objective of the test method was to quantify the energy absorption and identify the failure mechanisms associated with the observed frond formation in progressive crush testing of composite tubes. This was accomplished by testing composite plates under progressive crush load conditions.

A series of validation tests on representative composite material systems demonstrated that different damage mechanisms could be activated depending on the condition of the profile constraint. For example, in the braided material, the active damage mechanisms were localized crushing, fiber fracture on the tensile side of the specimen, and fiber buckling of the off-axis tows on the compressive side of the specimen. The fiber buckling was more extensive when the no constraint condition was used, whereas the fiber fracture was more predominant in the loose constraint tests.

**Table 3. Experimental Data for the Triaxial Braid O.**

| Specimen Number | Specimen Width (cm) | Profile Radius (cm) | Constraint | Initial Peak Load (N) | Max. Peak Load (N) | Sustained Crush Load (N) | SEA (J/g) | Avg. SEA (J/g) |
|---|---|---|---|---|---|---|---|---|
| O-1 | 3.814 | 0.635 | None | 4232.6 | 4421.1 | 1916.8 | 7.36 | |
| O-2 | 3.810 | 0.635 | None | 3673.7 | 3912.4 | 1000.9 | 6.91 | 7.32 |
| O-3 | 3.825 | 0.635 | None | 4967.0 | 4967.0 | 1238.2 | 7.69 | |
| O-4 | 3.814 | 0.635 | Loose | 3489.8 | 3489.8 | 2417.1 | 14.17 | |
| O-5 | 3.810 | 0.635 | Loose | 3365.7 | 3650.6 | 2934.2 | 20.24 | 17.23 |
| O-6 | 3.814 | 0.635 | Loose | 3434.2 | 3650.8 | 2745.3 | 17.28 | |

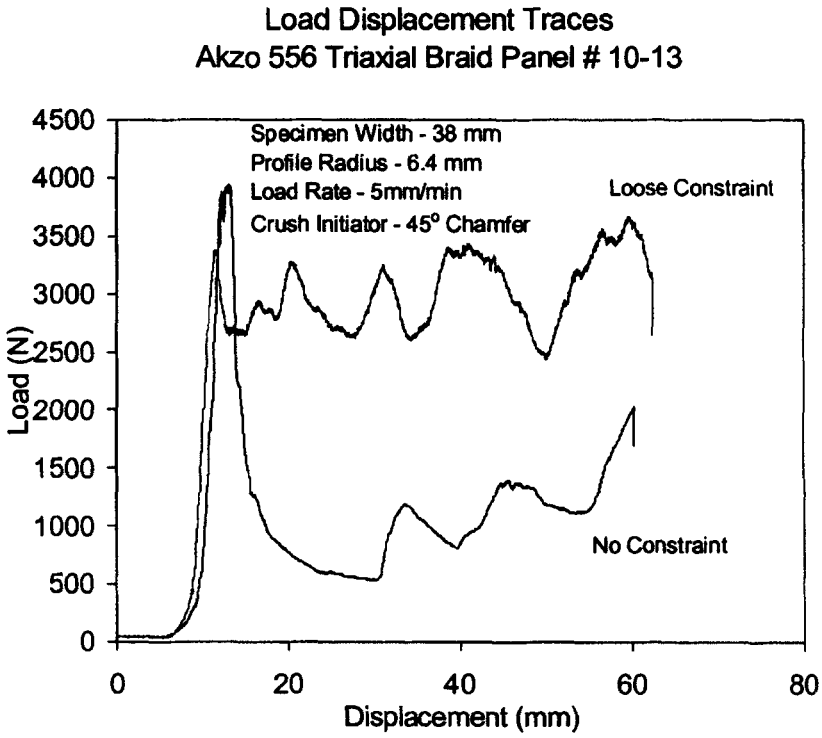


*Fig. 12. Load displacement traces for the triaxial braid O.*

Future testing will be conducted to quantify the effects of specimen width, profile radius, profile constraint and loading rate on the specific energy absorption and failure modes. The experimental data in conjunction with the test observations can be used to develop analytical models for predicting the crashworthiness of automotive composite structures.

## ACKNOWLEDGMENT

Research was sponsored by the U.S. Department of Energy, Assistant Secretary for Energy Efficiency and Renewable Energy, Office of Transportation Technologies, Lightweight Materials Program, under contract DE-AC05-00OR22725 with UT-Battelle, LLC.

## REFERENCES

1. D. Hull, *Sci. & Techn. Rev.*, **3**, 23 (1988).
2. D. Hull, *Comp. Sci. & Tech.*, **40**, 377 (1991).
3. G. L. Farley, *Proc. 43rd American Helicopter Society Annual Forum*, p. 63, St. Louis (1987).
4. G. L. Farley, *J. Comp. Mater.*, **20**, 390 (1986).
5. G. L. Farley, *J. Comp. Mater.*, **17**, 267 (1983).
6. G. L. Farley, *J. Comp. Mater.*, **20**, 322 (1986).
7. G. L. Farley, *Proc. of ICCM 6*, 3.57, F. L. Matthews, N. C. R. Buskell, J. M. Hodgkinson, and J. Mortan, eds., Elsevier Science Publishers Limited, London, UK (1987).
8. P. H. Thornton and P. J. Edwards, *J. Comp. Mater.*, **16**, 521 (1982).
9. D. Hull, *Structural Crashworthiness*, p. 118, N. Jones and T. Weirzbicki, eds., Butterworths, London (1983).
10. H. Hamada, S. Ramakrishna, Z. Maekawa, and M. Nakamura, *Proc. 10th Annual ASM/ESD Advanced Composite Conference*, p. 511, Dearborn, Michigan (1994).
11. D. W. Schmuesser and L. E. Wickliffe, *J. Engng. Mat. & Tech.*, **109**, 72 (1987).
12. H. Hamada and S. Ramakrishna, *J. Thermoplastic Composite Materials*, **9(3)**, 259 (1996).
13. G. L. Farley and R. M. Jones, *J. Comp. Mater.*, **26(1)**, 78 (1992).
14. G. L. Farley, *J. Comp. Mater.*, **26(3)**, 388 (1992).
15. P. H. Thornton, *J. Comp. Mater.*, **13**, 247 (1979).
16. C. H. Chiu, C. K. Lu, and C. M. Wu, *J. Comp. Mater.*, **31(22)**, 2309 (1997).
17. C. H. Chiu, C. K. Lu, and C. M. Wu, *Proc. of ICCM 10*, 4.187, B. C. Whistler, ed., Canada (1995).
18. S. Ramakrishna, H. Hamada, Z. Maekawa, and H. Sato, *J. Thermo. Comp. Mater.*, **8**, 323 (1995).
19. I. Y. Chang and J. K. Lees, *J. Thermo. Comp. Mater.*, **1**, 277 (1988).
20. I. Y. Chang, *Comp. Sci. & Techn.*, **24**, 61 (1985).
21. H. Satoh, H. Hirakawa, Z. Maekawa, H. Hamada, M. Nakamura, and D. Hull, *38th International SAMPE Symposium, Science of Advanced Materials and Process Engineering Series*, **38**, 952 (1993).
22. H. Hamada, J. C. Coppola, D. Hull, Z. Maekawa, and H. Sato, *Composites*, **23(4)**, 245 (1992).
23. G. L. Farley and R. M. Jones, *NASA TM-101634, AVSCOM TR-89-B-003* (1989).
24. D. Hull, *Proc. of ICCM-4*, p. 861, T. Hayashi, K. Kawata, and S. Umekawa, eds., Tokyo (1982).
25. J. P. Berry, *Energy Absorption and Failure Mechanisms of Axially Crushed GRP Tubes*, PhD thesis, University of Liverpool, U.K. (1984).
26. G. L. Farley, *27th SDM Conference* (1986).
27. G. L. Farley and R. M. Jones, *J. Comp. Mater.*, **26(12)**, 1741 (1992).
28. P. H. Thornton, J. J. Harwood, and P. Beardmore, *Comp. Sci. & Tech.*, **24**, 275 (1985).
29. D. D. Dubey and J. A. Vizzini, *J. Comp. Mater.*, **32**, 158 (1998).
30. H. Hamada, S. Ramakrishna, Z. Maekawa, M. Nakamura, and T. Nishiwaki, *Proc. 10th Annual ASM/ESD Advanced Composite Conference*, p. 523, Dearborn, Michigan (1994).
31. A. G. Mamalis, Y. B. Yuan, and G. L. Viegelahn, *Int. J. of Vehicle Design*, **13(5/6)**, 564 (1992).
32. A. H. Fairfull, *Scaling Effects in the Energy Absorption of Axially Crushed Composite Tubes*, PhD thesis, University of Liverpool, U.K. (1986).
33. A. H. Fairfull and D. Hull, *Proc. of ICCM 6*, 3.36, F. L. Matthews, N. C. R. Buskell, J. M. Hodgkinson, and J. Morton, eds., Elsevier Science and Publishers (1987).
34. G. L. Farley, *U.S. Army Research and Technology Activity—AVSCOM*, 1 (1989).
35. S. Ramakrishna and H. Hamada, *Key Engineering Materials*, **141–143**, 585 (1998).
36. S. Hanagud, J. I. Craig, P. Sriram, and W. Zhou, *J. Comp. Mater.*, **23**, 448 (1989).
37. H. Hamada, S. Ramakrishna, Z. Maekawa, and H. Sato, *J. Poly. & Poly. Comp.*, **3(2)**, 99 (1995).
38. S. Ramakrishna and D. Hull, *Comp. Sci. & Tech.*, **49**, 349, Elsevier Science Publishers Limited (1993).
39. S. Ramakrishna, *J. Reinf. Plast. & Comp.*, **14**, 1121 (1995).
40. P. Snowdon and D. Hull, *Proc. Fiber Reinforced Composites Conference '84*, 5.1, Plastics and Rubber Institute (1984).
41. P. H. Thornton, W. H. Tao, and R. E. Robertson, *Advanced Composite Materials: New Development and Applications Conference Proceedings*, p. 489, Detroit (1991).
42. D. C. Bannerman and C. M. Kindervater, *Proc. 4th International SAMPE European Chapter*, p. 155, Bordeaux, France (1984).
43. P. H. Thornton, *J. Comp. Mater.*, **24**, 594 (1990).
44. G. L. Farley, *J. Comp. Mater.*, **25**, 1314 (1991).
45. C. M. Kindervater, *National Specialists Meeting, Composite Structures of the American Helicopter Society*, Philadelphia (1983).
46. J. A. Lavoie and J. Morton, *NASA Contractor Report 4526* (1993).